Control of large 1D networks of double integrator agents: role of heterogeneity and asymmetry on stability margin

Technical Report

He Hao and Prabir Barooah

***Abstract*— We consider the distributed control of a network of heterogeneous agents with double integrator dynamics to maintain a rigid formation in 1D. The control signal at a vehicle is allowed to use relative position and velocity with its two nearest neighbors. Most of the work on this problem, though extensive, has been limited to homogeneous networks, in which agents have identical masses and control gains, and symmetric control, in which information from front and back neighbors are weighted equally. We examine the effect of heterogeneity and asymmetry on the closed loop stability margin, which is measured by the real part of the least stable eigenvalue. By using a PDE approximation in the limit of large number of vehicles, we show that heterogeneity has little effect while asymmetry has a significant effect on the stability margin. When control is symmetric, the stability margin decays to 0 as $1/N^2$, where N is the number of agents, even when the agents are heterogeneous in their masses and control gains. In contrast, we show that arbitrarily small amount of asymmetry in the velocity feedback gains can improve the decay of the stability margin to $O(1/N)$. Poor design of asymmetry makes the closed loop unstable for sufficiently large N. With equal amount of asymmetry in both velocity and position feedback gains, the closed loop is stable for arbitrary N. Effect of asymmetry in position feedback gains alone is an open problem. Numerical computations of the eigenvalues are provided that corroborate the PDE-based analysis.**

I. Introduction

In this paper we examine the closed loop dynamics of a system consisting of N interacting agents arranged in a line, where the agents are modeled as double integrators and each agent interacts with its two nearest neighbors through its local control action. This is a problem that is of primary interest to formation control applications, especially to platoons of vehicles, where the vehicles are modeled as point masses. An extensive literature exists on 1D automated platoons; see [1], [2], [3] and references therein. In the vehicular platoon problem, each vehicle tries to maintain a constant gap between itself and its two nearest neighbors. The desired trajectory of the entire network is available only to agent 1.

Although significant amount of research has been conducted on robustness-to-disturbance and stability issues of double integrator networks with decentralized control, most investigations consider the homogeneous case in which each agent has the same mass and employs the same controller (exceptions include [4], [5]). In addition, only symmetric control laws are considered in which the information from both the neighboring agents are weighted equally, with [6], [3] being exceptions. Khatir *et. al.* proposes heterogeneous control gains to improve string stability (sensitivity to disturbance) at the expense of control gains increasing without bound as N increases [4]. Middleton *et. al.* considers both unidirectional and bidirectional control, and concludes heterogeneity has little effect on the string stability under certain conditions on the the high frequency behavior [5]. On the other hand, [6] examines the effect of asymmetry (but not heterogeneity) on the response of the platoon as a result of sinusoidal disturbances in the lead vehicle, and concludes the asymmetry makes sensitivity to such disturbances worse.

In this paper we analyze the case when the agents are *heterogeneous* in their masses and control laws used, and also allow asymmetry in the use of front and back information. A decentralized *bidirectional* control law is considered that uses only relative position and relative velocity information from the two nearest neighbors. We examine the effect of heterogeneity and asymmetry on the stability margin of the closed loop, which is measured by the absolute value of the real part of the least stable pole. The stability margin determines the decay rate of initial formation keeping errors. Such errors arise from poor initial arrangement of the agents. The main result of the paper is that in a decentralized bidirectional control, heterogeneity has little effect on the stability margin of the overall closed loop, while even small asymmetry can have a significant impact. In particular, we show that in the symmetric case, the stability margin decays to 0 as $O(1/N^2)$, where N is the number of agents. We also show that the asymptotic trend of stability margin is not changed by agent-to-agent heterogeneity as long as the control gains do not have front-back asymmetry. On the other hand, arbitrary small amount of asymmetry in the way the local controllers use front and back information can improve the stability margin $O(1/N)$! To achieve such an improvement, each agent has to weigh relative velocity information from its front neighbor more heavily than the one behind it. In contrast, if more weight is given to the relative velocity information with the neighbor behind it, the closed loop becomes unstable if N is sufficiently large.

Most of the results in this paper are established by using a PDE approximation of the coupled system of ODEs that model the closed loop dynamics of the network. This is inspired by the work [3] that examined stability margin of

H. Hao and P. Barooah are with Department of Mechanical and Aerospace Engineering, University of Florida, Gainesville, FL 32611, USA hehao,pbarooah@ufl.edu. This work was supported by the National Science Foundation through Grant CNS-0931885 and by the Institute for Collaborative Biotechnologies through grant DAAD19-03-D-0004.

1D vehicular platoons in a similar framework. Compared to [3], this paper makes two novel contributions. First, we consider heterogeneous agents (the mass and control gains vary from agent to agent), whereas [3] consider only homogeneous agents. Secondly, [3] considered the scenario in which the desired trajectory of the platoon was one with a constant velocity, and moreover, every agent knew this desired velocity. In contrast, the control law we consider requires agents to know only the desired inter-agent separation; the overall trajectory information is made available only to agent 1. This makes the model more applicable to practical formation control applications in which the formation may be required to accelerate or decelerate occasionally, and the decision to do so is made solely by the lead agent. It was shown in [3] for the homogeneous formation that asymmetry in the position feedback can improve the stability margin from $O(1/N^2)$ to $O(1/N)$ while the absolute velocity feedback gain did not affect the asymptotic trend. In contrast, we show in this paper that with relative velocity and position feedback, asymmetry in the velocity feedback gain is the most significant determinant. It can lead to significant improvement in stability margin, or instability, depending on the design of the asymmetry. With equal amount of asymmetry in both position and velocity feedback, the closed loop is stable for arbitrary N, but it is not clear if improvement can be made on the stability margin by designing this asymmetry. Similarly, the effect of asymmetry in position feedback alone is left as an open question.

Although the PDE approximation is valid only in the limit $N \to \infty$, numerical comparisons with the original state-space model shows that the PDE model provides accurate results even for small N (5 to 10). PDE approximation is quite common in many-particle systems analysis in statistical physics and traffic-dynamics (see the article [7] for an extensive review.). The usefulness of PDE approximation in analyzing multi-agent coordination problems has been recognized also by researchers the controls community; see [8], [9], [3], [10] for examples. A similar but distinct framework based on partial *difference* equations has been developed by Ferrari-Trecate *et. al.* in [11]

The rest of this paper is organized as follows. Section II presents the problem statement and the main results of this paper. Section III describes the state-space and PDE models of the network of agents. Analysis and control design results together with their numerical corroboration appear in Sections IV and V, respectively. The paper ends with a discussion in Section VI.

II. Problem Statement and Main Results

A. Problem statement

We consider the formation control of N heterogeneous agents which are moving in 1D Euclidean space, as shown in Figure 1 (a). The position and mass of each agent are denoted by $p_i \in \mathbb{R}$ and m_i respectively. The mass of each agent is bounded, $|m_i - m_0|/m_0 \leq \delta$ for all i, where $m_0 > 0$ and $\delta \in [0, 1)$ are constants. The dynamics of each agent

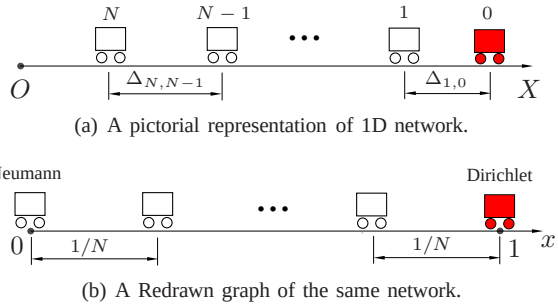

(a) A pictorial representation of 1D network.

(b) A Redrawn graph of the same network.

Fig. 1. Desired geometry of a network with N agents and 1 "reference agent", which are moving in 1D Euclidean space. The filled agent in the front of the network represents the reference agent, it is denoted by "0". (a) is the original graph of the network in the $p \in [0, \infty]$ coordinate and (b) is the redrawn graph of the same network in the $\tilde{p} \in [0, 1]$ coordinate.

are modeled as a double integrator:

$$m_i \ddot{p}_i = u_i, \tag{1}$$

where u_i is the control input (acceleration or deceleration command).

The information on the desired trajectory of the network is provided to agent 1. We introduce a *fictitious* reference agent with index 0 that perfectly tracks its desired trajectory, which is denoted by $p_0^*(t)$. Agent 1 is allowed to communicate with the reference agent. The desired geometry of the formation is specified by the *desired gaps* $\Delta_{i,i-1}$ for $i = 1, \ldots, N$, where $\Delta_{i,i-1}$ is the desired value of $p_{i-1}(t) - p_i(t)$. The control objective is to maintain a rigid formation, i.e., to make neighboring agents maintain their pre-specified desired gaps and to make agent 1 follow its desired trajectory $p_0^*(t) - \Delta_{1,0}$. Since we are only interested in maintaining rigid formations that do not change shape over time, $\Delta_{i,i-1}$'s are positive constants.

In this paper, we consider the following *decentralized* control law, whereby the control action at the i-th agent depends on i) the *relative position measurements* ii) the *relative velocity measurements* with its immediate neighbors in the formation:

$$\begin{aligned} u_i = &-k_i^f (p_i - p_{i-1} + \Delta_{i,i-1}) - k_i^b (p_i - p_{i+1} - \Delta_{i+1,i}) \\ &- b_i^f (\dot{p}_i - \dot{p}_{i-1}) - b_i^b (\dot{p}_i - \dot{p}_{i+1}), \quad i = 1, \ldots, N-1, \end{aligned} \tag{2}$$

where $k_{(.)}^f, k_{(.)}^b$ are the front and back position gains and $b_{(.)}^f, b_{(.)}^b$ are the front and back velocity gains respectively. For the agent with index N which does not have an agent behind it, the control law is slightly different:

$$u_i = -k_i^f (p_i - p_{i-1} + \Delta_{i,i-1}) - b_i^f (\dot{p}_i - \dot{p}_{i-1}). \tag{3}$$

Each agent i knows the desired gaps $\Delta_{i,i-1}$ and $\Delta_{i+1,i}$, while only agent 1 knows the desired trajectory $p_0^*(t)$ of the fictitious reference agent.

B. Main results

We formally define symmetric control and stability margin before stating the first main result.

Definition 1: The control law (2) is *symmetric* if each agent uses the same front and back control gains: $k_i^f = k_i^b, b_i^f = b_i^b$, for all $i \in \{1, 2, \ldots, N-1\}$.

Definition 2: The stability margin of a closed loop dynamics $\dot{x} = \mathbf{A}x$, which is denoted by S, is the absolute value of the real part of the least stable eigenvalue of $\mathbf{A}$.

Theorem 1: Consider an N-agent heterogeneous network with dynamics (1) and control law (2), (3), where the mass and the control gains of each agent satisfy $|m_i - m_0|/m_0 \leq \delta$, $|k_i^{(\cdot)} - k_0|/k_0 \leq \delta$ and $|b_i^{(\cdot)} - b_0|/b_0 \leq \delta$ where m_0, k_0 and b_0 are positive constants, and $\delta \in [0, 1)$ denotes the percent of heterogeneity. With symmetric control, the stability margin S of the network satisfies the following:

$$(1-2\delta)\frac{\pi^2 b_0}{8m_0}\frac{1}{N^2} \leq S \leq (1+2\delta)\frac{\pi^2 b_0}{8m_0}\frac{1}{N^2}, \qquad (4)$$

when $\delta \ll 1$. □

Numerical corroboration of the result is presented in Figure 3 in Section IV. The result above is also provable for an arbitrary $\delta < 1$ (not necessarily small) when there is only heterogeneity in mass using standard results on Strum-Louiville theory [12, Chapter 5]. For that case, the result is given in the following lemma and its proof is given in the end of the Appendix.

Lemma 1: Consider an N-agent heterogeneous network with dynamics (1) and control law (2), (3), where the mass and the control gains of each agent satisfy $0 < m_{\min} \leq m_i \leq m_{\max}$, $k_i^f = k_i^b = k_0$ and $b_i^f = b_i^b = b_0$, where m_0, k_0 and b_0 are positive constants. The stability margin S of the network satisfies the following:

$$\frac{\pi^2 b_0}{8m_{\max}}\frac{1}{N^2} \leq S \leq \frac{\pi^2 b_0}{8m_{\min}}\frac{1}{N^2}. \qquad (5)$$

□

The main implication of the result above is that *heterogeneity of masses and control gains plays no role in the asymptotic trend of the stability margin with N as long as the control gains are symmetric*. Note that the $O(1/N^2)$ decay of the stability margin described above has been shown for homogeneous platoons (all agents have the same mass and use the same control gains) independently in [13]. A similar result for homogeneous platoons with relative position and absolute velocity feedback was also established in [3].

The second main result of this work is that the stability margin can be greatly improved by introducing front-back asymmetry in the velocity-feedback gains. We call the resulting design *mistuning*-based design because it relies on small changes from the nominal symmetric gain b_0. In addition, a poor choice of such asymmetry can also make the closed loop unstable. Since heterogeneity is seen to have little effect, and for ease of analysis, we let $m_i = m_0$ in the sequel.

Theorem 2: For an N-agent network with dynamics (1) and control law (2), (3), with $m_i = m_0$ for all i, consider the problem of maximizing the stability margin by choosing the control gains with the constraint $|b_i^{(\cdot)} - b_0|/b_0 \leq \varepsilon$ for all i, with ε being a positive constant, and $k_i^{(f)} = k_i^{(b)} = k_0$. For vanishingly small values of ε, the following choice

$$b_i^f = (1+\varepsilon)b_0, \qquad b_i^b = (1-\varepsilon)b_0, \qquad (6)$$

results in the stability margin

$$S = \frac{\varepsilon b_0}{m_0}\frac{1}{N} + O(\frac{1}{N^2}). \qquad (7)$$

The formula is asymptotic in the sense that it holds when $N \to \infty$ and $\varepsilon \to 0$. In contrast, for the following choice of asymmetry

$$b_i^f = (1-\xi)b_0 \qquad b_i^b = (1+\xi)b_0, \qquad (8)$$

where $\xi \in (0, 1)$ is an arbitrary constant, the closed loop becomes unstable for sufficiently large N. □

The theorem says that with arbitrary small change in the front-back asymmetry, so that information from the front is weighted more heavily than the one from the back, the stability margin improves significantly. On the other hand, if information from the back is weighted more heavily than that from the front, the closed loop will become unstable if the network is large enough. It is interesting to note that the optimal gains turns out to be homogeneous.

The astute reader may inquire at this point what are the effects of introducing asymmetry in the position-feedback gains while keeping velocity gains symmetric, or introducing asymmetry in both position and velocity feedback gains. It turns out when equal asymmetry in both position and velocity feedback gains are introduced, the closed loop is stable for arbitrary N. We state the result in the next theorem.

Theorem 3: The closed loop dynamics of the N-agent network with the following asymmetry in control $k_i^f = (1+\rho)k_0$, $k_i^b = (1-\rho)k_0$, $b_i^f = (1+\rho)b_0$, $b_i^b = (1-\rho)b_0$, where ρ is a constant satisfying $\rho \in (-1, 1]$, are exponentially stable. □

The result above is for a equal amount (as a fraction of the nominal value) of asymmetry in the position feedback and velocity feedback gains. This constraint of equal asymmetry in position and velocity feedback is imposed in order to make the analysis tractable. Veerman proved a very similar result [6, Theorem 4.2], though the model was slightly different: the N-th agent's control law was $u_N = k^f(p_{N-1} - p_N) - b^f(\dot{p}_{N-1} - \dot{p}_N)$. Our proof (provided in the Appendix) follows a similar line of attack as [6, Theorem 4.2].

The analysis of the stability margin in the following cases are open problems: (i) unequal asymmetry in position and velocity feedback, (ii) velocity feedback gains are kept at their nominal symmetric values and asymmetry is introduced in the position feedback gains only.

III. Closed-loop dynamics: State-space and PDE models

A. State-space model of the network

Combining the open loop dynamics (1) with the control law (2), we get

$$m_i\ddot{p}_i = -k_i^f(p_i - p_{i-1} - \Delta_{i,i-1})$$

$$- k_i^b(p_i - p_{i+1} - \Delta_{i,i+1}) \\ - b_i^f(\dot{p}_i - \dot{p}_{i-1}) - b_i^b(\dot{p}_i - \dot{p}_{i+1}), \quad (9)$$

where $i \in \{1, \dots, N-1\}$. The dynamics of the N-th agent are obtained by combining (1) and (3), which are slightly different from (9). The desired trajectory of the i-th agent is $p_0^*(t) - \sum_{j=i}^{1} \Delta_{j,j-1} =: p_i^*(t)$. To facilitate analysis, we define the tracking error:

$$\tilde{p}_i := p_i - p_i^* \qquad \Rightarrow \qquad \dot{\tilde{p}}_i = \dot{p}_i - \dot{p}_i^*. \quad (10)$$

Substituting (10) into (9), and using $p_{i-1}^*(t) - p_i^*(t) = \Delta_{i,i-1}$, we get

$$m_i \ddot{\tilde{p}}_i = - k_i^f(\tilde{p}_i - \tilde{p}_{i-1}) - k_i^b(\tilde{p}_i - \tilde{p}_{i+1}) \\ - b_i^f(\dot{\tilde{p}}_i - \dot{\tilde{p}}_{i-1}) - b_i^b(\dot{\tilde{p}}_i - \dot{\tilde{p}}_{i+1}). \quad (11)$$

where we have used the fact that $\tilde{p}_0(t) \equiv 0$ since the trajectory of the reference agent is equal to its desired trajectory. By defining the state $\psi := [\tilde{p}_1, \dot{\tilde{p}}_1, \tilde{p}_2, \dot{\tilde{p}}_2, \cdots, \tilde{p}_N, \dot{\tilde{p}}_N]^T$, the closed loop dynamics of the network can now be written compactly from (11) as:

$$\dot{\psi} = \mathbf{A}\psi \quad (12)$$

where $\mathbf{A}$ is the closed-loop state matrix. In this paper, analysis and design is performed using a PDE approximation of the state space model (12), which is described next. The results are validated by numerical computations using the state-space model (12).

B. PDE model of the network

We now derive a continuum approximation of the closed loop dynamics (12) in the limit of large N, by following the steps involved in a finite-difference democratization in reverse. We define $k_i^{f+b} := k_i^f + k_i^b$, $k_i^{f-b} := k_i^f - k_i^b$, $b_i^{f+b} := b_i^f + b_i^f$, $b_i^{f-b} := b_i^f - b_i^b$. Substituting these into (11),

$$m_i \ddot{\tilde{p}}_i = \\ -\frac{k_i^{f+b} + k_i^{f-b}}{2}(\tilde{p}_i - \tilde{p}_{i-1}) - \frac{k_i^{f+b} - k_i^{f-b}}{2}(\tilde{p}_i - \tilde{p}_{i+1}) \\ -\frac{b_i^{f+b} + b_i^{f-b}}{2}(\dot{\tilde{p}}_i - \dot{\tilde{p}}_{i-1}) - \frac{b_i^{f+b} - b_i^{f-b}}{2}(\dot{\tilde{p}}_i - \dot{\tilde{p}}_{i+1}). \quad (13)$$

To facilitate analysis, we redraw the graph of the 1D network, so that the position error $\tilde{p}_i$ are defined in the interval $[0, 1]$, irrespective of the number of agents. The i-th agent in the "original" graph, is now drawn at position $(N-i)/N$ in the new graph. Figure 1 shows an example.

The starting point for the PDE derivation is to consider a function $\tilde{p}(x,t) : [0,1] \times [0, \infty) \to \mathbb{R}$ that satisfies:

$$\tilde{p}_i(t) = \tilde{p}(x,t)|_{x=(N-i)/N}, \quad (14)$$

such that functions that are defined at discrete points i will be approximated by functions that are defined everywhere in $[0,1]$. The original functions are thought of as samples of their continuous approximations. We formally introduce the following scalar functions $k^f(x), k^b(x), b^f(x), b^b(x)$ and $m(x) : [0,1] \to \mathbb{R}$ defined according to the stipulation:

$$k_i^{f \text{ or } b} = k^{f \text{ or } b}(x)|_{x=\frac{N-i}{N}}, \quad b_i^{f \text{ or } b} = b^{f \text{ or } b}(x)|_{x=\frac{N-i}{N}}, \quad (15)$$

and $m_i = m(x)|_{x=\frac{N-i}{N}}$. In addition, we define functions $k^{f+b}(x)$, $k^{f-b}(x)$, $b^{f+b}(x)$, $b^{f-b}(x) : [0,1]^D \to \mathbb{R}$ as

$$k^{f+b}(x) := k^f(x) + k^b(x), \quad k^{f-b}(x) := k^f(x) - k^b(x), \\ b^{f+b}(x) := b^f(x) + b^b(x), \quad b^{f-b}(x) := b^f(x) - b^b(x).$$

Due to (15), these satisfy

$$k_i^{f+b} = k^{f+b}(x)|_{x=(N-i)/N}, \quad k_i^{f-b} = k^{f-b}(x)|_{x=(N-i)/N} \\ b_i^{f+b} = b^{f+b}(x)|_{x=(N-i)/N}, \quad b_i^{f-b} = b^{f-b}(x)|_{x=(N-i)/N}.$$

To obtain a PDE model from (13), we first rewrite it as

$$m_i \ddot{\tilde{p}}_i = \frac{k_i^{f-b}}{N}\frac{(\tilde{p}_{i-1} - \tilde{p}_{i+1})}{2(1/N)} + \frac{k_i^{f+b}}{2N^2}\frac{(\tilde{p}_{i-1} - 2\tilde{p}_i + \tilde{p}_{i+1})}{1/N^2} \\ \frac{b_i^{f-b}}{N}\frac{(\dot{\tilde{p}}_{i-1} - \dot{\tilde{p}}_{i+1})}{2(1/N)} + \frac{b_i^{f+b}}{2N^2}\frac{(\dot{\tilde{p}}_{i-1} - 2\dot{\tilde{p}}_i + \dot{\tilde{p}}_{i+1})}{1/N^2}. \quad (16)$$

In the limit when $N \to \infty$, this can be seen as a finite difference discretization of the following PDE:

$$m(x)\Big(\frac{\partial^2}{\partial t^2}\Big)\tilde{p}(x,t) = \Big(\frac{k^{f-b}(x)}{N}\frac{\partial}{\partial x} + \frac{k^{f+b}(x)}{2N^2}\frac{\partial^2}{\partial x^2} + \\ \frac{b^{f-b}(x)}{N}\frac{\partial^2}{\partial x \partial t} + \frac{b^{f+b}(x)}{2N^2}\frac{\partial^3}{\partial x^2 \partial t}\Big)\tilde{p}(x,t). \quad (17)$$

The boundary conditions of PDE (17) depend on the arrangement of reference agent in the information graph. For our case, the boundary conditions are of the Dirichlet type at $x = 1$ where the reference agent is, and Neumann at $x = 0$:

$$\tilde{p}(1,t) = 0, \qquad \frac{\partial \tilde{p}}{\partial x}(0,t) = 0. \quad (18)$$

IV. Symmetric control

The starting point of our analysis is the investigation of the homogeneous and symmetric case: $m_i = m_0, k_i^{(\cdot)} = k_0, b_i^{(\cdot)} = b_0$ for some positive constants m_0, k_0, b_0, for $i \in \{1, \dots, N\}$. The analysis leading to the proof of Theorem 2 is carried out using the PDE model derived in the previous section. In the homogeneous and symmetric control case, using the notation introduced earlier, we get

$$m(x) = m_0, \\ k^{f+b}(x) = 2k_0, k^{f-b}(x) = 0, b^{f+b}(x) = 2b_0, b^{f-b}(x) = 0.$$

The PDE (17) simplifies to:

$$m_0 \frac{\partial^2 \tilde{p}(x,t)}{\partial t^2} = \frac{k_0}{N^2}\frac{\partial^2 \tilde{p}(x,t)}{\partial x^2} + \frac{b_0}{N^2}\frac{\partial^3 \tilde{p}(x,t)}{\partial x^2 \partial t}. \quad (19)$$

This is wave equation with Kelvin-Voight damping. Taking a Laplace transform w.r.t. the variable t of the above, we get

$$(m_0 s^2 - \frac{b_0 s + k_0}{N^2}\frac{\partial^2}{\partial x^2})\eta(s,x) = 0 \quad (20)$$

where $\eta(x,s)$ is the Laplace transform of $\tilde{p}(x,t)$. $\phi_\ell(x) = cos(\frac{2\ell-1}{2}\pi x)$ is the ℓ-th eigenfunction of the Laplacian $\frac{\partial^2}{\partial x^2}$ with the boundary condition $\eta(1,s)=0, \frac{\partial}{\partial x}\eta(0,s)=0$, which come from the boundary condition (18). The associated eigenvalues are

$$\lambda_\ell = \pi^2\frac{(2\ell-1)^2}{4}, \quad \ell = 1,2,\dots \tag{21}$$

Plugging the expansion $\eta(x,s)=\sum_{\ell=1}^{\infty}\phi_\ell(x)\beta_\ell(s)$, where β_ℓ are weights into (20), we get the characteristic equation $m_0 s^2 + \frac{b_0 s + k_0}{N^2}\lambda_\ell = 0$, so that the eigenvalues of the PDE are

$$s_\ell^{\pm} = -\frac{\lambda_\ell b_0}{2m_0N^2} \pm \frac{1}{2m_0N}\sqrt{\frac{\lambda_\ell^2 b_0^2}{N^2} - 4\lambda_\ell m_0 k_0} \tag{22}$$

For small ℓ and large N so that $N > (2\ell-1)\pi b_0/(4\sqrt{m_0k_0})$, the discriminant is negative, making the real part of the eigenvalues equal to $-\lambda_\ell b_0/(2m_0N^2)$. The least stable eigenvalue, the one closest to the imaginary axis, is obtained with $\ell = 1$:

$$s_1^{\pm} = -\frac{\pi^2 b_0}{8m_0}\frac{1}{N^2} \Rightarrow S = \frac{\pi^2 b_0}{8m_0N^2}. \tag{23}$$

We are now ready to present the proof of Theorem 1.

Proof of Theorem 1. Recall that in case of symmetric control we have

$$k_i^f = k_i^b, \quad b_i^f = b_i^b, \quad \forall i \in \{1,\dots,N\}.$$

In this case, using the notation introduced earlier, we have

$$k^{f-b}(x) = 0, \quad b^{f-b}(x) = 0,$$

The PDE (17) is simplified to:

$$m(x)\frac{\partial^2\tilde{p}(x,t)}{\partial t^2} = \frac{k^{f+b}(x)}{2N^2}\frac{\partial^2\tilde{p}(x,t)}{\partial x^2} + \frac{b^{f+b}(x)}{2N^2}\frac{\partial^3\tilde{p}(x,t)}{\partial x^2\partial t}, \tag{24}$$

The proof proceeds by a perturbation method. To be consistent with the bounds of the mass and control gains of each agent, let

$$\begin{aligned} m(x) &= m_0 + \delta\tilde{m}(x), \quad \tilde{m}(x) \in (-m_0, m_0] \\ k^{f+b}(x) &= 2k_0 + \delta\tilde{k}(x), \quad \tilde{k}(x) \in [-2k_0, 2k_0] \\ b^{f+b}(x) &= 2b_0 + \delta\tilde{b}(x), \quad \tilde{b}(x) \in [-2b_0, 2b_0]. \end{aligned}$$

where δ is a small positive number and $\tilde{m}(x), \tilde{k}(x), \tilde{b}(x)$ are the perturbation profiles. And let the perturbed eigenvalue be $s_\ell = s_\ell^{(0)} + \delta s_\ell^{(\delta)}$, the Laplace transform of $\tilde{p}(x,t)$ be $\eta = \eta^{(0)} + \delta\eta^{(\delta)}$, where $s_\ell^{(0)}$ and $\eta^{(0)}$ correspond to the unperturbed PDE (19). Eq. (49) provides the formula for $s_\ell^{(0)}$ (actually, $s_\ell^{\pm}$), and $\eta^{(0)}$ is the solution to (20). Taking a Laplace transform of PDE (24) with respect to t, plugging in the expressions for s_ℓ and η, and doing an $O(1)$ balance leads to the eigenvalue equation for the unperturbed PDE:

$$\mathcal{P}\eta^{(0)} = 0, \text{ where } \mathcal{P} := \left(m_0(s_\ell^{(0)})^2 - \frac{b_0 s_\ell^{(0)} + k_0}{N^2}\frac{\partial^2}{\partial x^2}\right)$$

Next we do an $O(\delta)$ balance, which leads to:

$$\begin{aligned} \mathcal{P}\eta^{(\delta)} = \Big(&- 2m_0 s_\ell^{(0)} s_\ell^{(\delta)}\eta^{(0)} - \tilde{m}(x)(s_\ell^{(0)})^2\eta^{(0)} \\ &+ \frac{\tilde{k}(x)}{2N^2}\frac{\partial^2\eta^{(0)}}{\partial x^2} + s_\ell^{(0)}\frac{\tilde{b}(x)}{2N^2}\frac{\partial^2\eta^{(0)}}{\partial x^2} + s_\ell^{(\delta)}\frac{b_0}{N^2}\frac{\partial^2\eta^{(0)}}{\partial x^2}\Big) =: R \end{aligned}$$

For a solution $\eta^{(\delta)}$ to exist, R must lie in the range space of the operator $\mathcal{P}$. Since $\mathcal{P}$ is self-adjoint, its range space is orthogonal to its null space. Thus, we have,

$$< R, \phi_\ell >= 0 \tag{25}$$

where ϕ_ℓ is also the ℓ^{th} basis vector of the null space of operator $\mathcal{P}$. We now have the following equation:

$$\begin{aligned} \int_0^1 \Big(&- 2m_0 s_\ell^{(0)} s_\ell^{(\delta)}\eta^{(0)} - \tilde{m}(x)(s_\ell^{(0)})^2\eta^{(0)} + \frac{\tilde{k}(x)}{2N^2}\frac{\partial^2\eta^{(0)}}{\partial x^2} \\ &+ s_\ell^{(0)}\frac{\tilde{b}(x)}{2N^2}\frac{\partial^2\eta^{(0)}}{\partial x^2} + s_\ell^{(\delta)}\frac{b_0}{N^2}\frac{\partial^2\eta^{(0)}}{\partial x^2}\Big)\phi_\ell dx = 0. \end{aligned}$$

Following straightforward manipulations, we got:

$$\begin{aligned} s_\ell^{(\delta)} =& \frac{b_0\lambda_\ell}{m_0^2N^2}\int_0^1 \tilde{m}(x)(\phi_\ell(x))^2dx \\ &- \frac{\lambda_\ell}{2m_0N^2}\int_0^1 \tilde{b}(x)(\phi_\ell(x))^2dx + \Im, \end{aligned} \tag{26}$$

where $\Im$ is an imaginary number when N is large ($N > (2\ell-1)\pi b_0/(4\sqrt{m_0k_0})$). Using this, and substituting the equation above into $s_\ell = s_\ell^{(0)} + \delta s_\ell^{(\delta)}$, and setting $\ell = 1$, we obtain the stability margin of the heterogeneous network:

$$\begin{aligned} S = \frac{b_0\pi^2}{8m_0N^2} &- \delta\frac{b_0\pi^2}{4m_0^2N^2}\int_0^1 \tilde{m}(x)\cos^2\left(\frac{\pi}{2}x\right)dx \\ &+ \delta\frac{\pi^2}{8m_0N^2}\int_0^1 \tilde{b}(x)\cos^2\left(\frac{\pi}{2}x\right)dx. \end{aligned}$$

Plugging the bounds $|\tilde{m}(x)| \le m_0$ and $|\tilde{b}(x)| \le 2b_0$, we obtain the desired result. ∎

A. Numerical comparison

We now present numerical computations that corroborates the PDE-based analysis. We consider the following mass and control gain profile:

$$\begin{aligned} k_i^f = k_i^b &= 1 + 0.2\sin(2\pi(N-i)/N), \\ b_i^f = b_i^b &= 0.5 + 0.1\sin(2\pi(N-i)/N), \\ m_i &= 1 + 0.2\sin(2\pi(N-i)/N). \end{aligned} \tag{27}$$

In the associated PDE model (24), this corresponds to $k^f(x) = k^b(x) = 1 + 0.2\sin(2\pi x)$, $b^f(x) = b^b(x) = 0.5 + 0.1\sin(2\pi x)$, $m(x) = 1 + 0.2\sin(2\pi x)$. The eigenvalues of the PDE, that are computed numerically using a Galerkin method with Fourier basis, are compared with that of the state space model to check how well the PDE model captures the closed loop dynamics. Figure 2 depicts the comparison of eigenvalues of the state-space model and the PDE model. It shows the eigenvalues of the state-space model is accurately approximated by the PDE model,

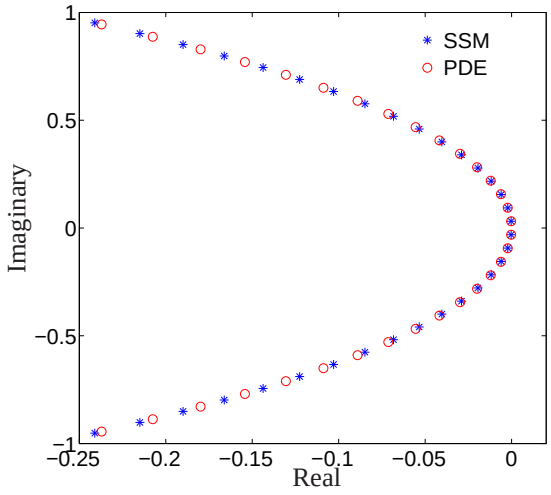

Fig. 2. Numerical comparison of closed-loop eigenvalues with symmetric control predicted by the state-space model (SSM) (12) and PDE model (24) with mixed Dirichlet-Neumann boundary conditions. Eigenvalues shown are for a network of 50 agents, and the mass and control gains profile are given in (27). Only a few eigenvalues are compared in the figure.

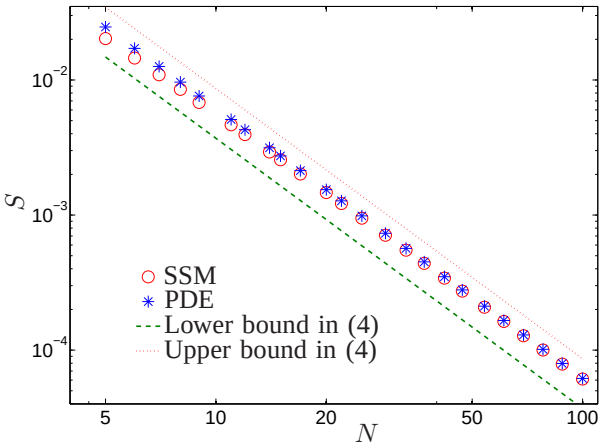

Fig. 3. The stability margin of the heterogeneous formation with symmetric control as a function of number of agents: the legends of SSM, PDE and lower bound, upper bound stand for the stability margin computed from the state space model, from the PDE model, and the asymptotic lower and upper bounds (5) in Theorem 1. The mass and control gains profile are given in (27).

especially the ones close to the imaginary axis. We see from Figure 3 that the closed-loop stability margin of the controlled formation is well captured by the PDE model. In addition, the plot corroborates the predicted bound (5).

V. Asymmetric control

We'll now develop the necessary tools to prove Theorem 2. With symmetric control, one obtains an $O(\frac{1}{N^2})$ scaling law for the stability margin because the coefficient of the $\frac{\partial^3}{\partial x^2 \partial t}$ term in the PDE (24) is $O(\frac{1}{N^2})$ and the coefficient of the $\frac{\partial^2}{\partial x \partial t}$ term is 0. Any asymmetry between the forward and the backward velocity gains will lead to non-zero $b^{f-b}(x)$ and a presence of $O(\frac{1}{N})$ term as coefficient of $\frac{\partial^2}{\partial x \partial t}$. By a judicious choice of asymmetry, there is thus a potential to improve the stability margin from $O(\frac{1}{N^2})$ to $O(\frac{1}{N})$. A poor choice of control asymmetry may lead to instability, as we'll show in the sequel.

We begin by considering the forward and backward feedback gain profiles

$$\begin{aligned} k^f(x) &= k_0, \quad k^b(x) = k_0, \\ b^f(x) &= b_0 + \varepsilon \tilde{b}^f(x), \quad b^b(x) = b_0 + \varepsilon \tilde{b}^b(x), \end{aligned} \tag{28}$$

where $\varepsilon > 0$ is a small parameter signifying the percent of asymmetry and $\tilde{b}^f(x)$, $\tilde{b}^b(x)$ are functions defined over $[0, 1]$ that capture velocity gain perturbation from the nominal value b_0. Define

$$\tilde{b}^s(x) := \tilde{b}^f(x) + \tilde{b}^b(x), \quad \tilde{b}^m(x) := \tilde{b}^f(x) - \tilde{b}^b(x). \tag{29}$$

Due to the definition of $k^{f+b}, k^{f-b}, b^{f+b}$ and b^{f-b}, we have

$$\begin{aligned} k^{f+b}(x) &= 2k_0, & k^{f-b}(x) &= 0, \\ b^{f+b}(x) &= 2b_0 + \varepsilon \tilde{b}^s(x), & b^{f-b}(x) &= \varepsilon \tilde{b}^m(x). \end{aligned}$$

The PDE (17) with homogeneous mass m_0 now becomes

$$\begin{aligned} m_0 \Big(\frac{\partial^2}{\partial t^2}\Big) \tilde{p}(x,t) &= \Big(\frac{k_0}{N^2} \frac{\partial^2}{\partial x^2} + \frac{b_0}{N^2} \frac{\partial^3}{\partial x^2 \partial t}\Big) \tilde{p}(x,t) \\ &+ \varepsilon \Big(\frac{\tilde{b}^s(x)}{2N^2} \frac{\partial^3}{\partial x^2 \partial t} + \frac{\tilde{b}^m(x)}{N} \frac{\partial^2}{\partial x \partial t}\Big) \tilde{p}(x,t). \end{aligned} \tag{30}$$

We now study the problem of how does the choice of the perturbations $\tilde{b}^s(x)$ and $\tilde{b}^m(x)$ (within limits so that the gains $b^f(x)$ and $b^b(x)$ are within pre-specified bounds) affect the stability margin. An answer to this question also helps in designing beneficial perturbations to improve the stability margin. The following result is used in the subsequent analysis.

Theorem 4: Consider the eigenvalue problem of the PDE (30) with mixed Dirichlet and Neumann boundary condition (18). The least stable eigenvalue is given by the following formula that is valid when $\varepsilon \to 0$ and $N \to \infty$:

$$\begin{aligned} s_1 = s_1^{(0)} &- \varepsilon \frac{\pi}{4m_0 N} \int_0^1 \tilde{b}^m(x) \sin(\pi x)\, dx \\ &- \varepsilon \frac{\pi^2}{8m_0 N^2} \int_0^1 \tilde{b}^s(x) \cos^2\big(\frac{\pi}{2} x\big)\, dx + \Im \end{aligned} \tag{31}$$

where $s_1^{(0)}$ is the least stable eigenvalue of the unperturbed PDE (19) with the same boundary conditions and $\Im$ is an imaginary number when N is large ($N > \pi b_0/(4\sqrt{m_0 k_0})$). □

Now we are ready to prove Theorem 2.

Proof of Theorem 2. It follows from Theorem 4 that to minimize the least stable eigenvalue, one needs to choose only $\tilde{b}^m(x)$ carefully. The reason is the second term involving $\tilde{b}^s(x)$ has the $O(1/N^2)$ trend. Therefore, we choose

$$\tilde{b}^s(x) \equiv 0.$$

This means that the perturbations to the "front" and "back" velocity gains satisfy:

$$\tilde{b}^f(x) = -\tilde{b}^b(x) \Leftrightarrow \tilde{b}^m(x) = 2\tilde{b}^f(x).$$

The most beneficial gains can now be readily obtained from Theorem 4. To minimize the least stable eigenvalue with $\tilde{b}^s(x) \equiv 0$, we should choose $\tilde{b}^m(x)$ to make the integral $\int_0^1 \tilde{b}^m(x)\sin(\pi x)dx$ as large as possible, which is achieved by setting $\tilde{b}^m(x)$ to be the largest possible value everywhere in the interval $[0,1]$. The constraint $|b_i^{(\cdot)} - b_0|/b_0 \leq \varepsilon$ translates to $b_0(1-\varepsilon) \leq b^{(\cdot)}(x) \leq b_0(1+\varepsilon)$, which means $\|\tilde{b}^f\|_\infty \leq b_0$ and $\|\tilde{b}^b\|_\infty \leq b_0$. With the choice of $\tilde{b}^s$ made above, we therefore have the constraint $\|\tilde{b}^m\| \leq 2b_0$. The solution to the optimization problem is therefore obtained by choosing $\tilde{b}^m(x) = 2b_0 \ \forall x \in [0,1]$. This gives us the optimal gains

$$\begin{aligned} &\tilde{b}^f(x) = b_0, && \tilde{b}^b(x) = -b_0, \\ \Rightarrow\ &b^f(x) = b_0(1+\varepsilon), && b^b(x) = b_0(1-\varepsilon). \end{aligned}$$

The least stable eigenvalue is obtained from Theorem (4):

$$s_1^+ = s^{(0)} - \frac{\varepsilon b_0}{m_0 N} - 0 + \Im.$$

Since $s^{(0)}$ is the least stable eigenvalue for the symmetric PDE, we know from Theorem 1 that $s^{(0)} = O(1/N^2)$. Therefore, it follows from the equation above that the stability margin is $S = Re(s_1^+) = \frac{\varepsilon b_0}{m_0 N} + O(\frac{1}{N^2})$. This proves the first statement of the theorem.

To prove the second statement, the control gain design $b_i^f = (1-\xi)b_0$ and $b_i^b = (1+\xi)b_0$ becomes $b^f(x) = (1-\xi)b_0$ and $b^b(x) = (1+\xi)b_0$. With this choice, it follows from Theorem (4) that

$$s_1^+ = s^{(0)} + \frac{\xi b_0}{m_0 N} - 0 + \Im.$$

Since $s^{(0)} = O(1/N^2)$, the second term, which is $O(1/N)$, will dominate for large N. Since this term is positive, the second statement is proved. ■

A. Comparison of stability margin computed from mistuned SSM and PDE

Figure 4 depicts the numerically obtained mistuned and nominal stability margins for both the PDE and state-space models. The nominal control gains are $k_0 = 1$, $b_0 = 0.5$, and the mistuned velocity gains used are the ones given by (6) in Theorem 2 with $\varepsilon = 0.1$. The figure shows that i) the closed-loop least stable eigenvalue match the PDE's accurately, even for small values of N; ii) the mistuned eigenvalues show large improvement over the symmetric case even though the velocity gains differ from their nominal values only by $\pm 10\%$. The improvement is particularly noticeable for large values of N, while being significant even for small values of N.

For comparison, the figure also depicts the asymptotic eigenvalue formula given in Theorem 2. The improvement in the stability margin with mistuning is remarkable even

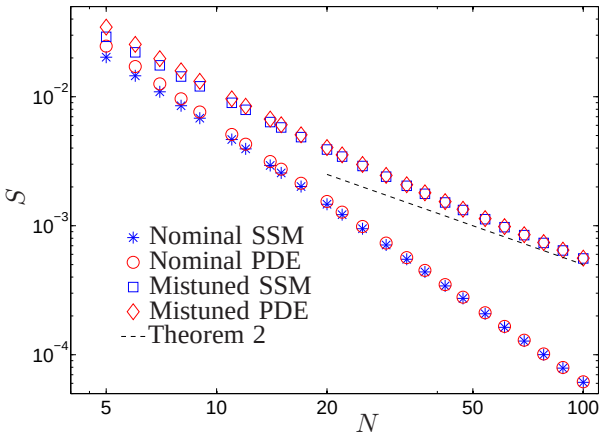

Fig. 4. Stability margin improvement by mistuning design. The nominal control gains are $k_0 = 1$, $b_0 = 0.5$, and the mistuned gains used are the ones given by (6) in Theorem 2 with $\varepsilon = 0.1$. The legends "Nominal SSM" and "Nominal PDE" stand for the stability margin computed from the state-space model and the PDE model, respectively, with symmetric control. The legends "Mistuned SSM" and "Mistuned PDE" stand for the stability margin computed from the state-space model and PDE model, respectively, with mistuned control.

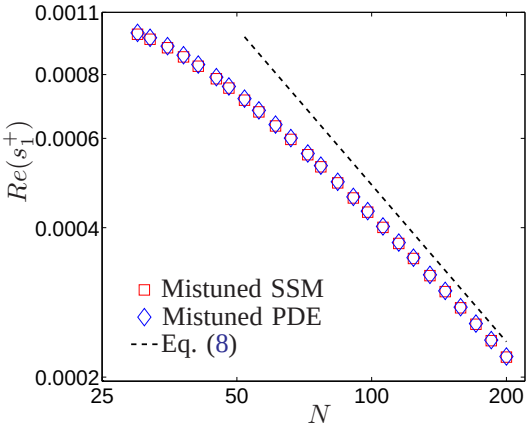

Fig. 5. The real part of the most unstable eigenvalues with poor asymmetry. The nominal control gains are $k_0 = 1$, $b_0 = 0.5$, and the mistuned gains used are the ones given by (8) in Theorem 2 with $\xi = 0.1$. The legends "Mistuned SSM" and "Mistuned PDE" stand for the stability margin computed from the state-space model and PDE model, respectively, with mistuned control.

the velocity gains are changed from their symmetric values by only $\pm 10\%$. Another interesting aspect of the result in Theorem 2 is that the improvement from $O(1/N^2)$ to $O(1/N)$ can be achieved by *arbitrarily small changes* to the nominal velocity gains.

Numerical validation that poor choice of asymmetry in control gains can lead to instability is shown in Figure 5. Note that the real part of these eigenvalues are positive and Eq. (8) makes an accurate prediction.

VI. Summary

We studied the role of heterogeneity and control asymmetry on the stability margin of a large $1D$ network of double-integrator agents. The control is decentralized; the control signal at every agent depends on the relative position and velocity measurements from its two nearest neighbors. It is shown that heterogeneity does not effect how the stability margin scales with N, the number of agents, whereas asymmetry plays a significant role. As long as control is symmetric, meaning information on relative position and velocity from both neighbors are weighed equally, agent-to-agent heterogeneity does not change the $O(1/N^2)$ scaling of stability margin. If front-back asymmetry is introduced in the velocity feedback gains, even by an arbitrarily small amount, the stability margin can be improved to $O(1/N)$. This is a significant improvement, especially for large N. In addition, the optimal asymmetric (mistuned) gain profile is quite simple to implement. With a maximum allowable variation of $\pm 10\%$ from the symmetric velocity gains, the optimal gains are obtained by letting the front gains to be 10 percent larger than the nominal gain and letting the back gains to be 10 percent smaller. If relative velocity information from the back neighbor is weighed more heavily than that from the front one, no matter how small the asymmetry is, the closed loop becomes unstable for sufficiently large N.

The general case of asymmetry in both position and velocity feedback gains is an open problem. Some preliminary answers are available in the special case when equal amount of asymmetry in both position and velocity feedback is introduced, which is parameterized by ρ. Then the closed loop is stable for arbitrary N, but the scaling laws of the stability margin with N is not known yet. Interestingly, it was shown by Veerman *et. al.* that in this special case, the sensitivity to disturbances is worse if ρ is other than 0. On the other hand, it was shown in [3] that asymmetry may help in reducing sensitivity to disturbance; though the scenario involved absolute position feedback. The effect of control asymmetry in sensitivity to disturbance therefore needs study.

References

[1] S. Darbha, J. K. Hedrick, C. C. Chien, and P. Ioannou, "A comparison of spacing and headway control laws for automatically controlled vehicles," *Vehicle System Dynamics*, vol. 23, pp. 597–625, 1994.

[2] P. Seiler, A. Pant, and J. K. Hedrick, "Disturbance propagation in vehicle strings," *IEEE Transactions on Automatic Control*, vol. 49, pp. 1835–1841, October 2004.

[3] P. Barooah, P. G. Mehta, and J. P. Hespanha, "Mistuning-based decentralized control of vehicular platoons for improved closed loop stability," *IEEE Transactions on Automatic Control*, vol. 54, no. 9, pp. 2100–2113, September 2009.

[4] M. E. Khatir and E. J. Davison, "Decentralized control of a large platoon of vehicles using non-identical controllers," in *Proceedings of the 2004 American Control Conference*, 2004, pp. 2769–2776.

[5] R. Middleton and J. Braslavsky, "String instability in classes of linear time invariant formation control with limited communication range, to appear," *IEEE Transactions on Automatic Control*, 2010.

[6] J. Veerman, "Stability of large flocks: an example," July 2009, arXiv:1002.0768.

[7] D. Helbing, "Traffic and related self-driven many-particle systems," *Review of Modern Physics*, vol. 73, pp. 1067–1141, 2001.

[8] A. Sarlette and R. Sepulchre, "A PDE viewpoint on basic properties of coordination algorithms with symmetries," in *48th IEEE Conference on Decision and Control*, December 2009, pp. 5139–5144.

[9] E. W. Justh and P. S. Krishnaprasad, "Steering laws and continuum models for planar formations," in *42nd IEEE Conference on Decision and Control*, December 2003, pp. 3609 – 3614.

[10] H. Hao, P. Barooah, and P. G. Mehta, "Distributed control of two dimensional vehicular formations: stability margin improvement by mistuning," in *ASME Dynamic Systems and Control Conference*, October 2009.

[11] G. Ferrari-Trecate, A. Buffa, and M. Gati, "Analysis of coordination in multi-agent systems through partial difference equations," *IEEE Transactions on Automatic Control*, vol. 51, no. 6, pp. 1058 – 1063, 2006.

[12] R. Haberman, *Elementary applied partial differential equations: with Fourier series and boundary value problems*. Prentice-Hall, 2003.

[13] J. Veerman, B. Stošić, and F. Tangerman, "Automated traffic and the finite size resonance," *Journal of Statistical Physics*, vol. 137, no. 1, pp. 189–203, October 2009.

[14] W. Yueh, "Eigenvalues of several tridiagonal matrices," *Applied Mathematics E-Notes*, vol. 5, pp. 66–74, 2005.

Appendix

Proof of Theorem 4. The proof proceeds by a perturbation method. Let the eigenvalues and Laplace transformation of $\tilde{p}(x,t)$ for the perturbed PDE (30) be $s_\ell = s_\ell^{(0)} + \varepsilon s_\ell^{(\varepsilon)}, \eta = \eta^{(0)} + \varepsilon \eta^{(\varepsilon)}$ respectively, where $s_\ell^{(0)}$ and $\eta^{(0)}$ are corresponding to the unperturbed PDE (19). Taking a Laplace transform of PDE (30), plugging in the expressions for s_ℓ and η, and doing an $O(\varepsilon)$ balance, which leads to:

$$\begin{aligned}\mathcal{P}\eta^{(\varepsilon)} =& s_\ell^{(0)} \frac{\tilde{b}^m(x)}{N} \frac{d\eta^{(0)}}{dx} + s_\ell^{(0)} \frac{\tilde{b}^s(x)}{2N^2} \frac{d^2\eta^{(0)}}{dx^2} \\ & - 2m s_\ell^{(0)} s_\ell^{(\varepsilon)} \eta^{(0)} + s_\ell^{(\varepsilon)} \frac{b_0}{N^2} \frac{d^2\eta^{(0)}}{dx^2} =: R\end{aligned}$$

For a solution $\eta^{(\varepsilon)}$ to exist, R must lie in the range space of the self-adjoint operator $\mathcal{P}$. Thus, we have,

$$< R, \phi_\ell >= 0$$

We now have the following equation:

$$\begin{aligned}\int_0^1 \Big(& s_\ell^{(0)} \frac{\tilde{b}^m(x)}{N} \frac{d\eta^{(0)}}{dx} + s_\ell^{(0)} \frac{\tilde{b}^s(x)}{2N^2} \frac{d^2\eta^{(0)}}{dx^2} \\ & -2m_0 s_\ell^{(0)} s_\ell^{(\varepsilon)} \eta^{(0)} + s_\ell^{(\varepsilon)} \frac{b_0}{N^2} \frac{d^2\eta^{(0)}}{dx^2} \Big) \phi_\ell dx = 0\end{aligned}$$

Following straightforward manipulations, we get:

$$\begin{aligned} m_0 (s_\ell^{(0)} + & \frac{b_0 \lambda_\ell}{2m_0 N^2}) s_\ell^{(\varepsilon)} = \\ & - s_\ell^{(0)} \frac{(2\ell-1)\pi}{4N} \int_0^1 \tilde{b}^m(x) \sin\left((2\ell-1)\pi x\right)\, dx \\ & - s_\ell^{(0)} \frac{(2\ell-1)^2\pi^2}{8N^2} \int_0^1 \tilde{b}^s(x) \cos^2\left(\frac{(2\ell-1)\pi}{2} x\right)\, dx. \end{aligned} \tag{32}$$

Substituting the equation above into $s_\ell = s_\ell^{(0)} + \varepsilon s_\ell^{(\varepsilon)}$, and set $\ell = 1$, we complete the proof. ∎

Proof of Theorem 3. With the control gains specified, it's straightforward to see that the state matrix $\mathbf{A}$ can be expressed in the following form,

$$\mathbf{A} = I_N \otimes A_1 + L \otimes A_2, \tag{33}$$

where I_N is the $N \times N$ identity matrix and $\otimes$ is the Kronecker product. And A_1, A_2 and L are defined as below

$$A_1 = \begin{bmatrix} 0 & 1 \\ 0 & 0 \end{bmatrix}, \quad A_2 = \begin{bmatrix} 0 & 0 \\ -k_0 & -b_0 \end{bmatrix}. \tag{34}$$

where k_0, b_0 are the nominal position and velocity gains respectively. L is the grounded graph *Laplacian*, which is specified as follows:

$$L = \begin{bmatrix} 2 & -1+\rho & & \\ -1-\rho & 2 & -1+\rho & \\ & \cdots & \cdots & \\ & -1-\rho & 2 & -1+\rho \\ & & -1-\rho & 1+\rho \end{bmatrix}. \tag{35}$$

From Schur's triangularization theorem, every square matrix is unitarily similar to an upper-triangular matrix. Therefore, there exists an unitary matrix U such that

$$U^{-1}LU = L_u,$$

where L_u is an upper-triangular matrix, whose diagonal entries are the eigenvalues of L. We now do a similarity transformation on matrix $\mathbf{A}$.

$$\begin{aligned} \bar{\mathbf{A}} :=& (U^{-1} \otimes I_2)\mathbf{A}(U \otimes I_2) \\ =& (U^{-1} \otimes I_2)(I_N \otimes A_1 + L \otimes A_2)(U \otimes I_2) \\ =& I_N \otimes A_1 + L_u \otimes A_2 \end{aligned}$$

It is a block upper-triangular matrix, and the block on each diagonal is $A_1 + \lambda_\ell A_2$, where $\lambda_\ell \in \sigma(L)$, where $\sigma(\cdot)$ denotes the spectrum (the set of distinct eigenvalues). Since similarity preserves eigenvalues, and the eigenvalues of a block upper-triangular matrix are the union of eigenvalues of each block on the diagonal, we have

$$\sigma(\mathbf{A}) = \sigma(\bar{\mathbf{A}}) = \bigcup_{\lambda_\ell \in \sigma(L)} \{\sigma(A_1 + \lambda_\ell A_2)\}, \tag{36}$$

$$= \bigcup_{\lambda_\ell \in \sigma(L)} \{\sigma \begin{bmatrix} 0 & 1 \\ -k_0\lambda_\ell & -b_0\lambda_\ell \end{bmatrix}\} \tag{37}$$

It follows now that the eigenvalues of $\mathbf{A}$ are the roots s of:

$$s^2 + \lambda_\ell b_0 s + \lambda_\ell k_0 = 0 \tag{38}$$

The ℓ-th eigenvalue λ_ℓ of the grounded graph Laplacian L is given by (see [14]),

$$\lambda_\ell = 2 - 2\sqrt{1-\rho^2}\cos\theta \tag{39}$$

where θ satisfies the following condition:

$$\sqrt{\frac{1+\rho}{1-\rho}}\sin(N+1)\theta = \sin N\theta, \text{ and } \theta \neq m\pi, m \in \mathbb{Z}.$$

It follows from (39) that $\lambda_\ell > 0$ for every ℓ, which shows that the coefficients of the second order characteristic equation (38) are positive. Hence, the eigenvalues of the state matrix $\mathbf{A}$ are in the left half plane, and thus the closed loop is exponentially stable. ■

Proof of Lemma 1. With the given profiles of thms and control gains, the PDE (17) simplifies to:

$$m(x)\frac{\partial^2 \tilde{p}(x,t)}{\partial t^2} = \frac{k_0}{N^2}\frac{\partial^2 \tilde{p}(x,t)}{\partial x^2} + \frac{b_0}{N^2}\frac{\partial^3 \tilde{p}(x,t)}{\partial x^2 \partial t}, \tag{40}$$

where $m_{\min} \leq m(x) \leq m_{\max}$. Taking a Laplace transform w.r.t. the variable t, we get

$$(m(x)s^2 - \frac{b_0 s + k_0}{N^2}\frac{\partial^2}{\partial x^2})\eta(s,x) = 0 \tag{41}$$

where $\eta(x,s)$ is the Laplace transform of $\tilde{p}(x,t)$.
Due to the linearity and homogeneity of the above PDE and boundary conditions, we are able to apply the method of separation of variables. We assume solution of the form $\eta(s,x) = \phi(x)h(s)$. Substituting the solution into (41) and dividing both sides by $\phi(x)h(s)$, we obtain:

$$\frac{s^2}{\frac{k_0}{N^2} + \frac{b_0}{N^2}s} = \frac{\phi''(x)}{m(x)\phi(x)} \tag{42}$$

Since each side of the above equation is independent from the other, so it's necessary for both sides equal to the same constant $-\lambda_\ell$. Then we have two separate equations:

$$\phi''(x) + \lambda_\ell m(x)\phi(x) = 0 \tag{43}$$

$$s^2 + \frac{b_0\lambda_\ell}{N^2}s + \frac{k_0\lambda_\ell}{N^2} = 0 \tag{44}$$

The spatial part solves the following regular Sturm-Liouville eigenvalue problem

$$\begin{aligned} \phi''(x) + \lambda_\ell m(x)\phi(x) = 0, \\ \frac{d\phi(0)}{dx} = \phi(1) = 0. \end{aligned} \tag{45}$$

The Rayleigh quotient is given by

$$\lambda_\ell = \frac{\int_0^1 (d\phi(x)/dx)^2 dx}{\int_0^1 \phi^2(x)m(x)dx}. \tag{46}$$

Plugging the inequality for $m(x)$, we have the following relation:

$$\frac{1}{m_{max}}\frac{\int_0^1 (d\phi(x)/dx)^2 dx}{\int_0^1 \phi^2(x)dx} \leq \lambda_\ell \leq \frac{1}{m_{min}}\frac{\int_0^1 (d\phi(x)/dx)^2 dx}{\int_0^1 \phi^2(x)dx}$$

Since we know the eigenvalue $\bar{\lambda}_\ell$ corresponding to Rayleigh quotient $\frac{\int_0^1 (d\phi(x)/dx)^2 dx}{\int_0^1 \phi^2(x)dx}$ is the eigenvalue obtained from (45) with $m(x) = 1$. And $\bar{\lambda}_\ell$ is given by

$$\bar{\lambda}_\ell = \frac{(2\ell-1)^2\pi^2}{4} \tag{47}$$

where ℓ is the wave number, $\ell = 1, 2, \ldots$.
It is straight forward to see that the least eigenvalue $\bar{\lambda}_\ell$ is obtain by setting $\ell = 1$, i.e. $\bar{\lambda}_1 = \pi^2/4$. So we have the following bounds for the least eigenvalue of λ_ℓ.

$$\frac{\pi^2}{4m_{max}} \leq \lambda_1 \leq \frac{\pi^2}{4m_{min}} \tag{48}$$

The eigenvalues of PDE (40) turn out to be the roots of the characteristic equation (44). The two roots of (44) are

$$s_\ell^{\pm} := \frac{-b_0\lambda_\ell/N^2 \pm \sqrt{b_0^2\lambda_\ell^2/N^4 - 4k_0\lambda_\ell/N^2}}{2}. \tag{49}$$

We call $s_\ell^{\pm}$ the ℓ-th pair of eigenvalues. The discriminant D in (49) is given by:

$$D := b_0^2\lambda_\ell^2/N^4 - 4k_0\lambda_\ell/N^2.$$

For large N and small ℓ, D is negative. So both the eigenvalues in (49) are complex, then the stability margin is only determined by the real parts of $s_\ell^{\pm}$. It follows from (49) that the least stable eigenvalues $s_{\min}$ (the ones closest to the imaginary axis) among them is the one that is obtained by minimizing λ_ℓ over ℓ. Then, this minimum is achieved at $\ell = 1$,

$$s_{\min} = s_1^{\pm},$$

and the real part is obtained

$$Re(s_{\min}) = -\frac{b_0\lambda_1}{2N^2}.$$

Following the definition of stability margin $S := |Re(s_{\min})|$ as well as the bounds for λ_1 given by (48), we complete the proof. ■